Photon counting statistics in single multi-level quantum system*

Wang Dong-Sheng(王东升) and Zheng Yu-Jun(郑雨军)†

School of Physics, Shandong University, Jinan 250100, *China*

(Received 16 November 2009; revised manuscript received 29 December 2009)

We theoretically study the statistics of photon emission of a single multi-level quantum system by employing the generating functions approach developed recently. The generalized decay constants are included in a single multi-level quantum system with quasi-degenerated levels in this work although they are normally neglected in the absence of (quasi-)degeneracies in a multi-level quantum system within the rotating wave approximation. The quantum beats, the line shapes and the Mandel's Q parameters, etc. are studied.

Keywords: photon statistics, generating function, single quantum system

PACC: 3280, 3200

1. Introduction

With the development of experimental techniques, it is possible to measure the photon emission from a single quantum system, such as a single molecule, atom or quantum dot.[1−6] The photon statistics, as a useful alternative to other approaches, could reveal important information on the single quantum system. Several different approaches, for example, the Monte Carlo method, the transfer matrix method and quantum jump approach, etc., are developed.[7−9] The generating function approach as a means to calculate the photon counting statistical observable of single quantum system has been developed recently.[10−31] This approach can capture both photon bunching and antibunching statistics within a single theoretical framework. Also, it provides the simple matter to calculate the high factorial moments, the probabilities for n photon emission and the distribution of the waiting time for emission event, etc. (see the following Eqs. (21), (22), and (26)).

The two-level system is an excellent model for the single molecule or quantum dot under the secular approximation. However, in some cases, the three-level or multi-level system should be considered for the quantum system. For example, the electron–hole pair states in quantum dot,[32,33] the hyperfine splitting in single atom[34−36] and the splitting of electromagnetically induced transparency (EIT) under the effect of magnetic field of ^{87}Rb, etc.[37−40] would be modeled via the single multi-level quantum system. The generating function has been used to study the related questions, for example, the influence of spectral diffusion on single molecule photon statistics and the control of photon emission of single molecules in a solid matrix, etc.[19−27,41−43] However, these studies have neglected the generalized decay constants (GDCs) based on the secular approximation. Namely, the non-degeneracy condition is met in previous studies. For the single multi-level quantum system with (quasi-)degenerated states, the secular approximation will fail. In this case, the generalized decay constants cannot be neglected again, and they will serve to mediate the coherence between the spontaneous emission paths.

In this work, we generally consider the photon emission statistics for the single multi-level quantum system with (quasi-)degenerated states under the continuous wave (cw) excitation by a single monochromatic external field. Specifically, we investigate the line shapes and the Mandel's Q parameters and the quantum beats (QBs) for single multi-level quantum system with (quasi-)degenerated states. The purpose of this work is twofold. First, we generally extend the generating function approach to the single multi-level quantum system with quasi-degenerated levels. We include the generalized decay constants which are normally neglected in non-degenerate system. Secondly,

*Project supported by the National Natural Science Foundation of China (Grant Nos. 10674083 and 10874102), partially by the Research Fund for the Doctoral Program of Higher Education (Grant No. 200804220004), and Wang acknowledges the support from the National Found for Fostering Talents of Basic Science (NFFTBS) (Grant No. J0730318).

†Corresponding author. E-mail: yzheng@sdu.edu.cn

© 2010 Chinese Physical Society and IOP Publishing Ltd

we investigate the effects caused by quantum interference and quantum coherence, and it will be shown that the generating function approach can capture the quantum effects in the usual approximation: Markov approximation, independent rates of variation and neglect of frequency shift.

This paper is arranged as follows. In Section 2, we give the concise process to extend the generating function approach to the single multi-level quantum system with quasi-degenerated levels including the generalized decay constants and briefly review the formula to extract the information of photon statistics from the formulism of the generating function. In Section 3, we present the numerical results for a seven-level quantum system with single ground state and six quasi-degenerated excited states. We consider several cases of quantum beats (QBs), the line shapes and the Mandel's Q parameters. In Section 4, we give a brief conclusion.

2. Theoretical framework

We generally consider the single quantum system with the $\mathcal{N}$ quasi-degenerated ground states (denoted as $|G\rangle$) and the $\mathcal{M}$ quasi-degenerated excited states (denoted as $|E\rangle$). The schematic diagram of the system we considered in the work is shown in Fig. 1. As usual, we assume that the system can have dipole transitions between the ground state $|G\rangle$ and excited state $|E\rangle$, but the transitions between the quasi-degenerated states in $|G\rangle$ or $|E\rangle$ are dipole forbidden. The dynamical evolution of the single multi-level quantum system driven by the external semiclassical laser field can be described via the Liouville equation[1]

$$\mathrm{i}\hbar\frac{\partial\rho}{\partial t}=[\mathcal{H}(t),\rho], \tag{1}$$

where $\mathcal{H}$ is the Hamiltonian of the system. The Hamiltonian could be written as

$$\mathcal{H}(t)=\mathcal{H}_{\mathrm{S}}+\mathcal{H}_{\mathrm{R}}+\mathcal{H}_{\mathrm{SR}}+\mathcal{H}_{\mathrm{L}}(t), \tag{2}$$

where

$$\mathcal{H}_{\mathrm{S}} = \sum_{n}\hbar\omega_n|n\rangle\langle n|, \tag{3}$$

$$\mathcal{H}_{\mathrm{R}} = \sum_{\boldsymbol{k}\lambda}\hbar\omega_{\boldsymbol{k}\lambda}\left(a^{\dagger}_{\boldsymbol{k}\lambda}a_{\boldsymbol{k}\lambda}+\frac{1}{2}\right), \tag{4}$$

$$\mathcal{H}_{\mathrm{SR}} = -\mathrm{i}\sum_{nm;\boldsymbol{k}\lambda}\hbar g^{(nm)}_{\boldsymbol{k}\lambda}(a_{\boldsymbol{k}\lambda}-a^{\dagger}_{\boldsymbol{k}\lambda})|n\rangle\langle m|, \tag{5}$$

$$\mathcal{H}_{\mathrm{L}}(t) = -\boldsymbol{\mu}\cdot\boldsymbol{\mathcal{E}_0}(t)\cos\omega_{\mathrm{L}}t, \tag{6}$$

and

$$g^{(nm)}_{\boldsymbol{k}\lambda}=\sqrt{\frac{\omega_{\boldsymbol{k}\lambda}}{2\varepsilon_0 V\hbar}}\,\boldsymbol{\mu}_{nm}\cdot\boldsymbol{e}_{\boldsymbol{k}\lambda}. \tag{7}$$

With the notations, $\mathcal{H}_{\mathrm{S}}$ is the Hamiltonian of the quantum system, $\mathcal{H}_{\mathrm{R}}$ is the Hamiltonian of the quantized radiative field, $\mathcal{H}_{\mathrm{SR}}$ is the Hamiltonian of the interaction between the quantum system and the radiative field, and $\mathcal{H}_{\mathrm{L}}$ is the Hamiltonian of the interaction between the quantum system and the external semiclassical laser field $\boldsymbol{\mathcal{E}}(t)=\boldsymbol{\mathcal{E}}_0(t)\cos\omega_{\mathrm{L}}t$. $\boldsymbol{\mathcal{E}}_0(t)$ is the polarization of the laser field with frequency of ω_{L}. $\boldsymbol{\mu}$ is the vector of the dipole moment operator for the system with matrix elements $\boldsymbol{\mu}_{ge}=\langle g|\boldsymbol{\mu}|e\rangle$. $a_{\boldsymbol{k}\lambda}$ and $a^{\dagger}_{\boldsymbol{k}\lambda}$ are the annihilation and creation operators for a photon of wavevector $\boldsymbol{k}$, polarization λ and frequency $\omega_{\boldsymbol{k}\lambda}$. ε_0 is the permittivity, $\hbar$ is Planck's constant, and V is the volume of the cubic cavity considered in determining the modes of the radiation field.

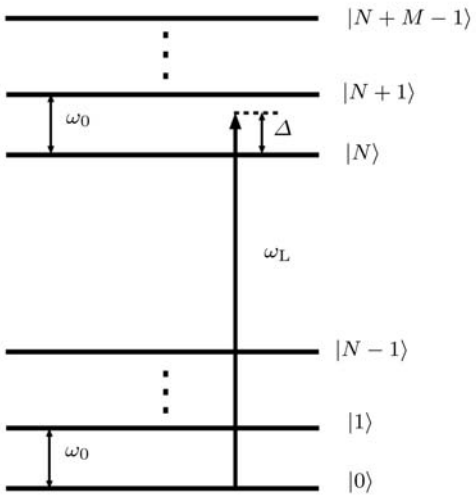


Fig. 1. The schematic diagram of the single multi-level quantum system studied in this work.

Since we are interested in the dynamical evolution of the single multi-level quantum system, the evolution for the reduced density matrix of the system $\sigma(t)\equiv\mathrm{Tr}_{\mathrm{R}}\{\rho(t)\}$ is considered. The evolution of the reduced density matrix can be written as[1]

$$\dot{\sigma}_{ij}(t)=\mathcal{L}_{ij,kl}\sigma_{kl}. \tag{8}$$

We hereafter define the notations for the specification of the elements in $\mathcal{L}_{ij,kl}$

$$\omega_{kl} = \omega_k-\omega_l, \tag{9}$$

$$\gamma_{ijkl} = \boldsymbol{\mu}_{ij}\cdot\boldsymbol{\mu}_{kl}\frac{|\omega_{kl}|^3}{6\varepsilon_0\hbar\pi c^3}. \tag{10}$$

Equation (8) can, after we partition the Liouville operator into two parts: $\mathcal{L}^{(0)}_{ij;kl}$ and $\mathcal{L}^{(+)}_{ij;kl}$, be written as

$$\dot{\sigma}_{ij}(t) = \mathcal{L}^{(0)}_{ij,kl}\sigma_{kl} + \mathcal{L}^{(+)}_{ij,kl}\sigma_{kl}, \tag{11}$$

where we define[44−47]

$$\begin{aligned}
&\mathcal{L}^{(0)}_{ij,kl}\sigma_{kl} \\
&= -\mathrm{i}\omega_{ij}\sigma_{ij} + \frac{1}{i\hbar}\boldsymbol{\mathcal{E}}_0(t) \\
&\cdot \sum_{a=0}^{\mathcal{N}+\mathcal{M}-1} (\boldsymbol{\mu}_{aj}\sigma_{ia} - \boldsymbol{\mu}_{ia}\sigma_{aj})\cos\omega_{\mathrm{L}}t \\
&- \sum_{e=\mathcal{N}}^{\mathcal{N}+\mathcal{M}-1}\sum_{g=0}^{\mathcal{N}-1} \gamma_{igge}\sigma_{ej} \\
&- \sum_{e'=\mathcal{N}}^{\mathcal{N}+\mathcal{M}-1}\sum_{g'=0}^{\mathcal{N}-1} \gamma_{e'g'g'j}\sigma_{ie'},
\end{aligned} \tag{12}$$

and

$$\mathcal{L}^{(+)}_{ij,kl}\sigma_{kl} = 2\sum_{e,e'=\mathcal{N}}^{\mathcal{N}+\mathcal{M}-1} \gamma_{eije'}\sigma_{ee'}. \tag{13}$$

The elements of $\mathcal{L}^{(+)}_{ij;kl}$ reflect the spontaneous emission of photons and the virtual photon transitions.

Although the photon statistics can be obtained from the solution of Eq. (11) in terms of an iterative expansion in $\mathcal{L}^{(+)}_{ij;kl}$, it is convenient to proceed by defining the generating function. The generating function takes the form[14−16]

$$\mathcal{G}(s,t) = \sum_{n=0}^{\infty}\sigma^{(n)}(t)s^n, \tag{14}$$

where s is called the counting variable, $\sigma^{(n)}(t)$ is that portion of the reduced density matrix stemming from the system with the prior history of n photon emission events, and

$$\sigma(t) = \sum_{n=0}^{\infty}\sigma^{(n)}(t). \tag{15}$$

The evolution equations of the matrices of generating function can, within rotating wave approximation (RWA) and dipole approximation, be obtained as follows:

$$\begin{aligned}
\dot{\mathcal{G}}_{gg'} &= -\mathrm{i}\omega_{gg'}\mathcal{G}_{gg'} \\
&\quad + \frac{\mathrm{i}}{2}\sum_{e=\mathcal{N}}^{\mathcal{N}+\mathcal{M}-1}(\Omega_{eg'}\mathcal{G}_{ge} - \Omega_{ge}\mathcal{G}_{eg'}) \\
&\quad + 2s\sum_{e,e'=\mathcal{N}}^{\mathcal{N}+\mathcal{M}-1}\gamma_{egg'e'}\mathcal{G}_{ee'}, \\
\dot{\mathcal{G}}_{ee'} &= -\mathrm{i}\omega_{ee'}\mathcal{G}_{ee'} + \frac{\mathrm{i}}{2}\sum_{g=0}^{\mathcal{N}-1}(\Omega_{ge'}\mathcal{G}_{eg} - \Omega_{eg}\mathcal{G}_{ge'}) \\
&\quad - \sum_{e''=\mathcal{N}}^{\mathcal{N}+\mathcal{M}-1}(\Gamma_{ee''}\mathcal{G}_{e''e'} + \Gamma_{e''e'}\mathcal{G}_{ee''}), \\
\dot{\mathcal{G}}_{ge} &= -\mathrm{i}\Delta\mathcal{G}_{ge} + \frac{\mathrm{i}}{2}\sum_{g'=0}^{\mathcal{N}-1}\Omega_{g'e}\mathcal{G}_{gg'} \\
&\quad - \frac{\mathrm{i}}{2}\sum_{e'=\mathcal{N}}^{\mathcal{N}+\mathcal{M}-1}\Omega_{ge'}\mathcal{G}_{e'e} - \sum_{e'=\mathcal{N}}^{\mathcal{N}+\mathcal{M}-1}\Gamma_{ee'}\mathcal{G}_{ge'},
\end{aligned} \tag{16}$$

where $\Omega_{ge} = \boldsymbol{\mu}_{ge}\cdot\boldsymbol{\mathcal{E}}_0(t)/\hbar$ is the Rabi frequency for the external field, and $\Delta = \omega_{\mathrm{L}} - \omega_{eg}$ is the detuning frequency. g (g') and e (e') are used to label the quasi-degenerated states (from $|0\rangle$ to $|\mathcal{N}-1\rangle$) in the ground state $|G\rangle$ and the quasi-degenerated states (from $|\mathcal{N}\rangle$ to $|\mathcal{N}+\mathcal{M}-1\rangle$) in the excited state $|E\rangle$, respectively.

We used the shorthand in Eq. (16)

$$\Gamma_{ee'} \equiv \sum_{g=0}^{\mathcal{N}-1}\gamma_{egge'}. \tag{17}$$

It should be noted that $\mathcal{G}_{gg'}$=$\mathcal{G}^*_{g'g}$, $\mathcal{G}_{ee'}$=$\mathcal{G}^*_{e'e}$, and $\mathcal{G}_{ge}$=$\mathcal{G}^*_{eg}$ in Eq. (16).

For convenience, we hereafter use the shorthand notations as follows:

$$\gamma_e \equiv \gamma_{egge}, \tag{18}$$

$$\gamma_{ee'} \equiv \gamma_{egge'}. \tag{19}$$

The working generating function $\mathcal{Y}(s,t)$ for photon emission events is defined by

$$\mathcal{Y}(s,t) = \sum_{k=0}^{\mathcal{N}+\mathcal{M}-1}\mathcal{G}_{kk}(s,t). \tag{20}$$

We can extract the statistical quantities related to photon emission from the working generating function Eq. (20). For example, the factorial moments of photon emission can be calculated via

$$\begin{aligned}
&\langle N^{(m)}\rangle(t) \\
&\equiv \langle N(N-1)\cdots(N-m+1)\rangle(t) \\
&= \frac{\partial^m}{\partial s^m}\mathcal{Y}(s,t)|_{s=1},
\end{aligned} \tag{21}$$

and the probability of photon emission is as follows:

$$\mathcal{P}_n(t) = \frac{1}{n!}\frac{\partial^n}{\partial s^n}\mathcal{Y}(s,t)|_{s=0}, \tag{22}$$

etc.

The Mandel's Q parameter can reflect the fluctuation of the photon emission process, which is bunching when $Q > 0$, and anti-bunching when $-1 < Q < 0$. It is well defined as

$$Q = \frac{\langle N^{(2)}\rangle - \langle N^{(1)}\rangle^2}{\langle N^{(1)}\rangle}. \tag{23}$$

The absorption line shape is obtained by

$$I(\omega_{\rm L}) = \frac{\rm d}{{\rm d}t}\langle N^{(1)}\rangle(t) \tag{24}$$

for long time.

The intensity $I(t)$ is

$$I(t) = \frac{\rm d}{{\rm d}t}\langle N^{(1)}\rangle(t)\mid_{\omega_{\rm L}}. \tag{25}$$

Also, the distribution of the waiting time for emission event can be obtained[48]

$$\mathcal{W}(t) = -\frac{\partial}{\partial t}\mathcal{Y}(s,t)|_{s=0}. \tag{26}$$

3. Numerical results

In this section we study the quantum beats, the line shapes and the Mandel's Q parameter of the single multi-level quantum system using the theoretical framework shown in the previous section. In many cases, we should study the multi-level system instead of the two-level system or the three-level system, for example, the hyperfine multi-level single atom,[34,35] the effect of magnetic field on the electromagnetically induced transparency (EIT) of ^{87}Rb,[40] etc. to capture the more exact dynamical process. As Cardimona *et al.*[44,45] have shown, some effects in simple system, such as the "dark state", are not expected in multi-level system. Also the photon statistics in multi-level system has not yet been studied well.[25,27] To make connection with previous work,[25,44] here we consider the single seven-level quantum system with single ground state (namely, $\mathcal{N}=1$) and six quasi-degenerated excited states (namely, $\mathcal{M}=6$). In the following, we denote $\boldsymbol{\mu}_{eg}=\boldsymbol{\mu}_e$ $(e=1,2,\ldots,\mathcal{M})$ since the system we considered here has single ground state. This system has symmetrical structure of the excited states, so when driven by the continuous wave laser field or by the vacuum field under different structures of the dipole moments, there should be some kind of dynamical symmetry within. For the seven-level quantum system, we consider three different cases corresponding to different values of the generalized decay constants (GDCs):

Case 1 All the dipole moments are parallel. Thus, all the GDCs exist.

Case 2 The adjacent dipole moments are orthogonal. That is, the dipole moments $\boldsymbol{\mu}_1$, $\boldsymbol{\mu}_3$, and $\boldsymbol{\mu}_5$ are parallel (we denote this as group #1), $\boldsymbol{\mu}_2$, $\boldsymbol{\mu}_4$, and $\boldsymbol{\mu}_6$ (we denote this as group #2) are also parallel, but the dipole moments of the two groups, #1 and #2, are orthogonal.

Case 3 Similar with Case 2, but the group #1 includes the dipole moments $\boldsymbol{\mu}_1$, $\boldsymbol{\mu}_2$ and $\boldsymbol{\mu}_3$, and the group #2 includes the dipole moments $\boldsymbol{\mu}_4$, $\boldsymbol{\mu}_5$ and $\boldsymbol{\mu}_6$.

The main purpose considered for the above three cases is that the different coherent natures of the quantum system through the lineshapes and the Mandel's Q parameters could be shown well. The information of the system, for example, the characters of the structures of the (quasi-degenerated) states or the orientations of the dipole moments, would be represented via the lineshapes and higher factorial moments.

It will been seen that GDCs play the important role in the dynamical evolution of single quantum systems. The "sub-beats" can be caused from GDCs. It is due to the GDCs that the photon emission process and the statistical behaviours of emission photon show the "spectral diversity". It is clear that the role of GDCs cannot be captured within the secular approximation.[46]

3.1. Quantum beats

The quantum beats (QBs) is a simple but important quantum phenomenon, which refers to the oscillation of the intensity of emitted photon from the quantum system due to the quantum coherence. In our numerical calculations, we assume that the seven-level system consists of a single ground state and six equally spaced excited states, we refer to the parameter in Refs. [25] and [49]. We demonstrate that, due to the interaction within the excited states, there exists different behaviour from the two or three level system.

3.1.1. All the dipole moments are parallel

In this case, to present the nature of the quantum beats in the seven-level quantum system, three different initial conditions are chosen.

(i) The single excited state as the initial condition

For this type of initial conditions, there exist six choices from state $|1\rangle$ to state $|6\rangle$. The results of the intensity and the Mandel's Q parameter are shown in Fig. 2 (the top panel). The interesting thing is that the quantum beats show the symmetry about the centre of the excited states. Namely, the results of the initial states $|1\rangle$, $|2\rangle$ or $|3\rangle$ are the same with the results of initial states $|6\rangle$, $|5\rangle$ or $|4\rangle$, respectively. Also, the

quantum beats show the "step" effects due to the couplings between the state chosen as the initial state and the other states. The QBs in top panel of Fig. 2 show some kind of subsidiary beats in each "step". Our calculations show that the subsidiary beats are related to the degree of (quasi-)degeneracy of the system (i.e., the numbers of subsidiary beats equal the degree of (quasi-)degeneracy of the system minus one). For example, for the case of the initial state $|1\rangle$, shown as the solid line in Fig. 2, the up panel, there are five subsidiary beats between each "step" since the degree of (quasi-)degeneracy of the system is six. The difference of the quantum beats for the different single initial state origins from the difference of the coupling of coherence through the generalized decay constant $\gamma_{ee'}$.

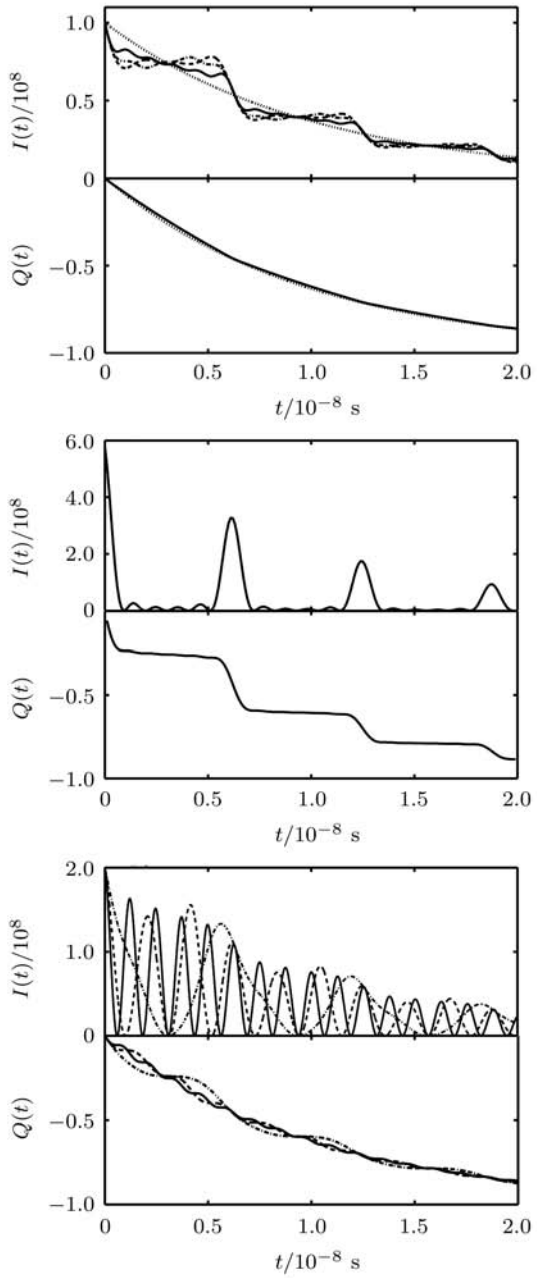


Fig. 2. The intensities and the Mandel's Q parameters (Case 1). Top panel is for the single excited state as the initial condition: $|1\rangle$ (solid lines), $|2\rangle$ (dashed-dot lines), $|3\rangle$ (dashed lines). We only show the Mandel's Q parameter for the initial condition $|1\rangle$ for clarity. (When the dipole moment of the chosen initial state is orthogonal to the others, there is no quantum beats. The result is plotted using dotted lines.) Middle panel: the superposition of all excited states $\sum_{e=1}^{6}|e\rangle/\sqrt{6}$ as the initial condition. Bottom panel: the initial condition is chosen as the superposition of two excited states: $(|1\rangle+|6\rangle)/\sqrt{2}$ (solid lines), $(|2\rangle+|5\rangle)/\sqrt{2}$ (dashed lines), and $(|3\rangle+|4\rangle)/\sqrt{2}$ (dashed-dot lines). The parameters are: $\omega_0 = 10\times10^8$ s^{-1}, $\gamma_e = 0.05\ \omega_0$ $(e=1,\ldots,6)$, all the other GDCs are taken as $0.05\ \omega_0$.

Moreover, if the dipole moment of the chosen initial state is orthogonal to the dipole moments of all the other states, the ways of all the coupling between this state and the other states should be turned off (i.e., $\gamma_{ee'}=0$). If this happened, there will be no quantum beats. The intensity and the Mandel's Q parameter will simply decay exponentially in time as shown by dotted-lines in the top panel of Fig. 2. The Mandel's Q parameter goes to minus one eventually as there is no external driven field.

The photon fluctuation, shown as the Mandel's Q parameter, does not show much oscillation as the figure shows. This is due to the fact that the photon emission process is dominated only by one excited state, and the process is mediated by other excited states since part of the population is transferred to other excited states during the emission. However, this is not the same with the other cases below.

(ii) The superposition of all quasi-degenerated excited states as the initial condition

The result of this case is shown in the middle panel of Fig. 2. Similar with the above case, the sub-beats are also shown among the "main" sharp peaks. The Mandel's Q parameter shows the "step". The intensity peaks are of the same position with the decreasing of the Mandel's Q parameter. Also, there are five zero points of the intensity between the "main" peaks. This is consistent with the above case. For the sub-beats between the "main" peaks, we attribute it to the coupling of coherence of the quasi-degenerated levels in excited states $|E\rangle$. In other words, these sub-beats form a kind of "gap" in which the intensity is nearly zero. The coupling of the coherence within the excited states turns to inhibit the emission process.

(iii) The superposition of two excited states as the initial condition

As noted before, the QBs for the system show the symmetry about the centre of the excited states. For a deeper understanding of this symmetry, we choose the symmetric superpositions of two excited states as the initial conditions. Namely, we use $|\Psi(0)\rangle = (|1\rangle + |6\rangle)/\sqrt{2}$, $|\Psi(0)\rangle = (|2\rangle + |5\rangle)/\sqrt{2}$, or $|\Psi(0)\rangle = (|3\rangle + |4\rangle)/\sqrt{2}$. We can see that the ratio of the numbers of the peaks of QBs for the three initial conditions within each period is $5:3:1$, which shows in the bottom panel of Fig. 2 clearly. This ratio is consistent with the ratio of the energy spacing of the chosen states, namely, the ratio of the energy spacing between the chosen states is $\omega_{61}:\omega_{52}:\omega_{43} = 5:3:1$ ($\omega_{ee'} = \omega_e - \omega_{e'}$ is the energy spacing between the excited states $|e\rangle$ and $|e'\rangle$).

3.1.2. The adjacent dipole moments are orthogonal

For this case, we consider two initial conditions.

(I) The superposition of three excited states in group #1 as the initial states, namely, $|\Psi(0)\rangle = (|1\rangle + |3\rangle + |5\rangle)/\sqrt{3}$

The results of the intensity and the Mandel's Q parameter are shown in Fig. 3 (the dashed lines). The figure shows clearly that there is only one sub-beat peak within a period of QBs. As we noted before, the coherence ways between group #1 and group #2 are to turn off all the couplings between them since two groups have the orthogonal dipole moments. The quantum beats just occur within the states in group #1. Based on this analysis, if we choose the superposition of three states in group #2 as the initial condition, the system should present the same nature since the system has the symmetry about the centre of the excited states. This has been confirmed by our calculations (we do not plot this out in the figure).

(II) The superposition of all states in group #1 and part states in group #2

For this initial condition, we choose the initial condition $|\Psi(0)\rangle = (|1\rangle + |3\rangle + |5\rangle)/\sqrt{4} + |6\rangle/\sqrt{4}$. The results of the intensity and the Mandel's Q parameter are plotted using the solid lines in Fig. 3. They would have similar natures with former initial condition. The only difference is that the peak heights of quantum beats are smaller than that in the former since the partition of group #1, in this case, is small. And, the heights of the sub-beats become higher due to the contributions of the state $|6\rangle$. The reason is that the state $|6\rangle$ can cause the quantum interference between the states $|2\rangle$, $|4\rangle$ and $|6\rangle$ in group #2 since the state $|6\rangle$ is chosen as the partial initial condition. The results of QBs caused from state $|6\rangle$ in group #2 are also shown in Fig. 3 using dashed-dot lines.

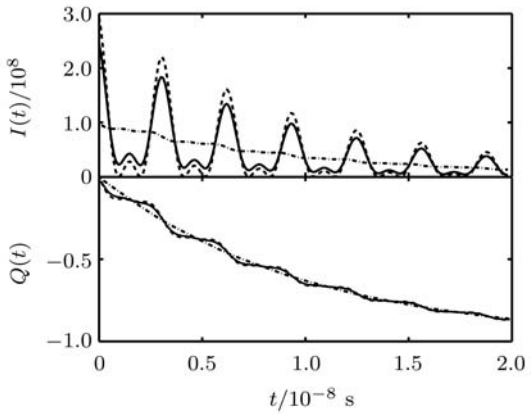


Fig. 3. The intensities and the Mandel's Q parameters (Case 2). The parameters are: $\omega_0 = 10 \times 10^8$ s^{-1}, all the GDCs are 0.05 ω_0 except $\gamma_{ee'} = 0$ ($e = 1, 3, 5$; $e' = 2, 4, 6$). The dashed line is for the initial condition $(|1\rangle + |3\rangle + |5\rangle)/\sqrt{3}$. The solid line is for the initial condition $(|1\rangle + |3\rangle + |5\rangle + |6\rangle)/\sqrt{4}$. The dashed-dot line is for the initial condition $|6\rangle$.

3.1.3. Similar with Case 2, but the group #1 includes the dipole moments μ_1, μ_2 and μ_3, and the group #2 includes the dipole moments μ_4, μ_5, and μ_6

In order to see the effects of energy spacing between the states in the same group, we consider another case in this subsection. That is, we set the states $|1\rangle$, $|2\rangle$ and $|3\rangle$ in group #1, and the states $|4\rangle$, $|5\rangle$ and $|6\rangle$ in group #2. The dipole moments of the two groups are also orthogonal. The only difference between this case and the case 2 is the energy spacing between the states in the same group. We choose the similar initial conditions with the former cases, namely, we use three different initial conditions: $|\Psi(0)\rangle = (|1\rangle + |2\rangle + |3\rangle)/\sqrt{3}$, $|\Psi(0)\rangle = (|1\rangle + |2\rangle + |3\rangle)/\sqrt{4} + |6\rangle/\sqrt{4}$, and $|\Psi(0)\rangle = |6\rangle$. The results are plotted in Fig. 4. In this case, the energy spacing is ω_0, which is the half of the energy spacing in the former case. From Fig. 4, we can see that the nature of the system is similar with Case 2 but not the numbers of the peaks of QBs or the frequency of QBs. It is definite that the frequency of QBs is half of that in Case 2 since the energy spacing is half of that in Case 2. The results in Fig. 4 demonstrated this point.

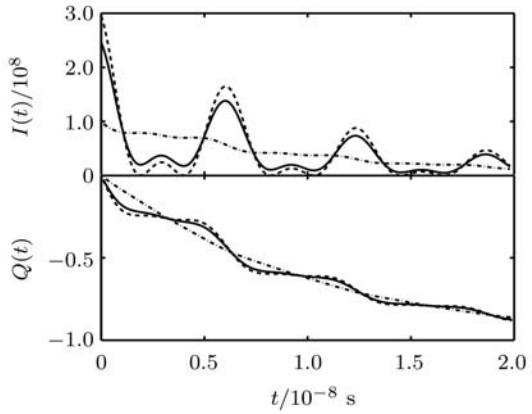


Fig. 4. The intensities and the Mandel's Q parameters (Case 3). The parameters are: $\omega_0 = 10 \times 10^8$ s^{-1}, all the GDCs are 0.05 ω_0 except $\gamma_{ee'} = 0$ ($e = 1, 2, 3$; $e' = 4, 5, 6$). The dashed line is for the initial condition $(|1\rangle + |2\rangle + |3\rangle)/\sqrt{3}$. The solid line is for the initial condition $(|1\rangle + |2\rangle + |3\rangle + |6\rangle)/\sqrt{4}$. The dashed-dot line is for the initial condition $|6\rangle$.

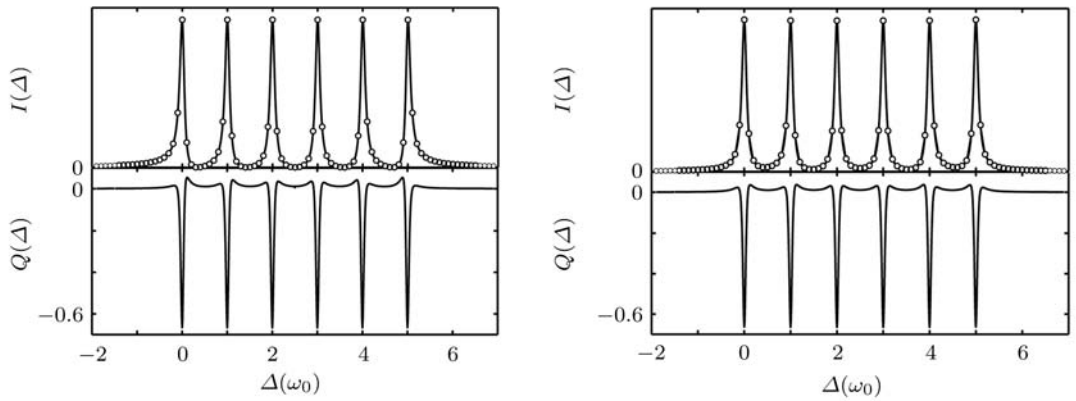
3.2. Driven by continuous wave (cw) laser field

In this subsection, we report the study for the statistical natures of photon emission of the single seven-level quantum system driven by external continuous wave (cw) laser field. We calculate the line shapes and the Mandel's Q parameter for the system. Generally, the structures of line shapes and the Mandel's Q parameters can be affected by the strengths of the external field and the orientations of the dipole moments. The three different strengths of driven laser field are considered: the weak ($\Omega = 0.05\omega_0$), medium ($\Omega = 0.5\omega_0$) and strong ($\Omega = 2.5\omega_0$) driven laser field.

3.2.1. All the dipole moments are parallel

The line shapes $I(\Delta)$ and the Mandel's $Q(\Delta)$ parameters for different strengths of driven laser field are shown in the left column of Fig. 5. For comparison with previous results, we use the identical parameters with Ref. [44]. We also plot the line shapes of Cardimona, Raymer and Stroud, Jr obtained from the dressed state method.[44] From Fig. 5, we can find that there exists the complete absence of absorption for the resonance of laser detuning. The most interesting thing is the symmetry of the line shapes for this seven-level quantum system. That is, the complete absences of absorption are symmetric about the centre of the excited states (i.e., $\Delta = 2.5\omega_0$). Also, the positions of the absence of absorption show the "blue shifts" (the detuning frequency is higher than the centre of the excited states or $\Delta > 2.5\omega_0$) or "red shifts" (the detuning frequency is lower than the centre of the excited states or $\Delta < 2.5\omega_0$). Our calculations show that the values of the detuning frequencies are equal to $0.337\omega_0$, $1.426\omega_0$, $2.500\omega_0$, $3.574\omega_0$, $4.663\omega_0$, respectively. Clearly, these shifts show the symmetry about the centre $\Delta = 2.5\omega_0$, too. The absorption peaks also show the similar shift, which is becoming obvious with the increasing of the laser intensity. It is shown in the left column of Fig. 5. While the natural linewidth is much more narrower than the energy spacing of the excited states (in the work, we choose $\gamma = 0.05\omega_0$), we should not expect absorption broaden under weak exciting (see the top panel of left column in Fig. 5 for the weak field $\Omega = 0.05\omega_0$). However, it is not the case when the intensity of the external field becomes strong. The power broadening would broaden the peaks. The results for the medium and strong field are shown in the middle and bottom panels of left column in Fig. 5 respectively.

Since all the six dipole moments of excited states are parallel, in this case, the so-called "dark state" can be induced. Or, there exists the complete absence absorption between the excited states. The number



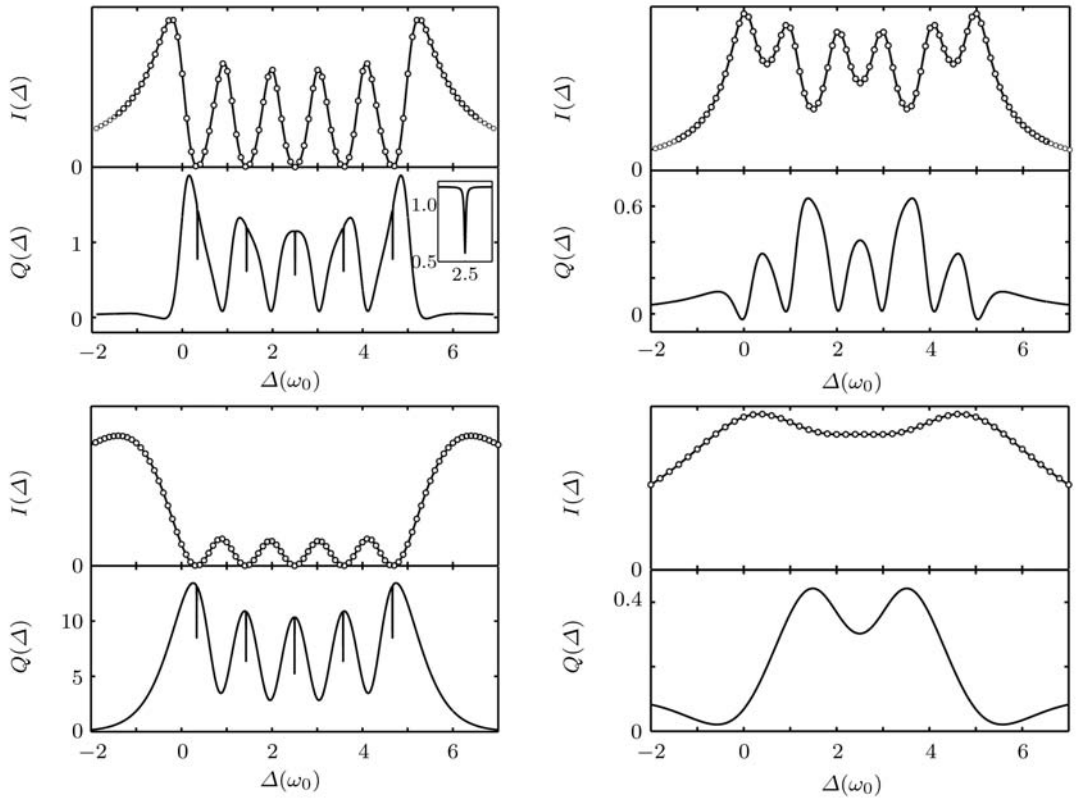


Fig. 5. The line shapes and the Mandel's Q parameters for the seven-level system. The left column is for the case of dipole moments parallel (Case 1), all the GDCs are 0.05 ω_0. The right column is for the case of the adjacent dipole moments parallel (Case 2), all the GDCs are 0.05 ω_0 except $\gamma_{ee'} = 0$ ($e = 1, 3, 5$; $e' = 2, 4, 6$). The Rabi frequencies are 0.05 ω_0 for top row, 0.5 ω_0 for middle row, and 2.5 ω_0 for bottom row. The initial condition is $|\Psi(0)\rangle = |0\rangle$. The circles are the results of dressed state approach.[44]

of complete absorption in this case is five since the degree of (quasi-)degeneracy of the seven-level system is six. Generally, there should be $\mathcal{M} - 1$ dark states if the degree of the degeneracy of the excited states is $\mathcal{M}$. As discussed above, the "dark" states are not located in the centre of the adjacent states and the detuning frequencies shift away the centre of excited states with the symmetry.

The emission photon shows anti-bunching corresponding to each resonant transition under weak exciting. What we should pay attention to is that there are five small "holes" between each sharp drops for the Q spectra. This corresponds to the zero points of the line shape. The holes can be viewed as the sign of the existence of the dark states. The reason is that the couplings between the different coherences serve to mediate the relative contribution. Also, it has been demonstrated in our former work.[25] As the intensity increases, the five holes on the Q spectra get more distinct. The clarification of the width of the narrow hole is shown in the inset of the left middle panel in Fig. 5 for the medium strength of the driving laser field.

3.2.2. The adjacent dipole moments are orthogonal

To compare with Case 1, we consider a different case, namely, the adjacent dipole moments are orthogonal. In this case, the coupling pathways of absorption via GDCs are turned off since the adjacent dipole moments are orthogonal. Once the interference ways are turned off, the dark states or the complete absence of absorption would disappear. The results are shown in the top, middle and bottom panels of the right column in Fig. 5 for three different strengths of driven laser field, respectively. The line shapes of this case were studied by Cardimona, Raymer and Stroud, Jr,[44] their results obtained from the dressed state method are also plotted in the figure with circles. Although the line shapes and the Mandel's Q parameters show the similar natures in this case and Case 1 for the weak driven field, we can also see that there is no complete absence of absorption in this case. What is more, for the medium and strong driven field, the line shapes and the Mandel's Q parameters have obvious different natures with the corresponding cases of the

dipole moments parallel. The figure shows that there are no "narrow holes" of the Mandel's Q spectra for the medium and strong driving field. In strong exciting regime, the system undergoes the similar process with the case of medium strength of driven field except that there will be no definite interference structures as shown in the bottom panel of right column in Fig. 5. The value of the Mandel's Q parameter is positive through all the detuning regime for the strong driving field in this case, which shows the super-Poissonian behaviours.

The line shapes and the Mandel's Q parameters are not obviously affected by the changes of the dipole moment orientations for the weak driving laser field. However, with the increases of the strength of the laser field, the differences between the parallel and the orthogonal cases become apparent.

3.2.3. Similar with Case 2, but the group #1 includes the dipole moments μ_1, μ_2 and μ_3, and the group #2 includes the dipole moments μ_4, μ_5, and μ_6

The results of the line shapes and the Mandel's Q parameters as the function of the detuning frequency Δ and the Rabi frequency Ω are plotted in Fig. 6. In this case, the interesting point we should notice is the behaviours of the system under different intensities of external field for the detuning frequency Δ between $2\omega_0$ and $3\omega_0$. From Fig. 6, we can see that the two peaks of the line shape profile at $\Delta = 2\omega_0, 3\omega_0$ "go" together with the increasing of the driving laser field. This "motion" of the peaks causes a "hill", and it corresponds to a "valley" for the Mandel's Q spectra. Physically, the power broadening will cause to broaden of the interference peaks of the states in the same group (group #1 or #2). We have the big values by the simple addition of this broaden at the regime of the detuning frequency $2\omega_0 \sim 3\omega_0$ (the reason is that the dipole moments are orthogonal between the groups #1 and #2, and the coherence pathway is turned off). To compare with the former case, the line shapes and the Mandel's Q parameters of three strengths of the driving laser field $0.05\omega_0$, $0.5\omega_0$ and $2.5\omega_0$ are plotted using bold dashed-dot lines in the figure.

As the intensity of driving laser field goes up, the peaks of the line shapes at $\Delta = 1\omega_0, 2\omega_0, 3\omega_0, 4\omega_0$ move into together, and the Mandel's Q spectra are becoming similar varieties, too. In addition, there are no holes in Q spectra and zero points on the line shape, that is to say the dark state can not be induced in this case.

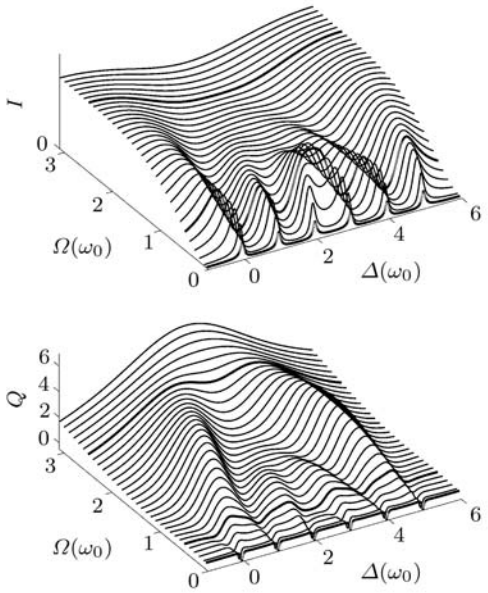


Fig. 6. The line shapes and Mandel's Q parameters as the function of the detuning frequencies and the Rabi frequencies (Case 3). The parameters are: all the GDCs are 0.05 ω_0 except $\gamma_{ee'} = 0$ ($e = 1, 2, 3$; $e' = 4, 5, 6$). The three strengths of the driving laser field 0.05 ω_0, 0.5 ω_0 and 2.5 ω_0 are plotted using bold dashed-dot lines. The initial condition is $|\Psi(0)\rangle = |0\rangle$.

3.3. Three-level-like V-type system

The seven-level system could be translated to the three-level-like V-type system by extending the separation of states $|3\rangle$ and $|4\rangle$. Under strong driven laser or pulse fields, the hyperfine splitting of the states in the three-level system could affect the dynamics, for instance, the splitting of the electromagnetically induced transparency (EIT) of ^{87}Rb,[40] etc. In our simulation, we make connection with our previous work.[25] The separation of states $|3\rangle$ and $|4\rangle$ is, in our calculation, chosen ten times as the separation of other states (i.e., $\omega_{34} = 10\omega_0$). After doing this, the seven-level system could be thought as the V-type three-level system with the quasi-degeneracy (the degree of quasi-degeneracy is 3) in each excited state, and we note them as state $|\mathcal{E}_1\rangle$ (including levels $|1\rangle$, $|2\rangle$, and $|3\rangle$) and state $|\mathcal{E}_2\rangle$ (including levels $|4\rangle$, $|5\rangle$, and $|6\rangle$), respectively. In our calculations, we assume the dipole moments in state $|\mathcal{E}_1\rangle$ (or $|\mathcal{E}_2\rangle$) are parallel. We can investigate this three-level-like V-type system using the same theoretical procedure. The results of the line shapes and the Mandel's Q parameters are plotted in Fig. 7. In contrast with the three-level system we studied before,[25] the line shapes and the Mandel's Q

parameters show the structures as expected. The left column of Fig. 7 shows the case of the parallel dipole moments of the states $|\mathcal{E}_1\rangle$ and $|\mathcal{E}_2\rangle$. As we noted, in this case, there is the complete absence of absorption at the centre (i.e., $\Delta = 7\omega_0$ here). The interesting thing about the line shapes for the three-level-like system is also the complete absence of absorption in the states $|\mathcal{E}_1\rangle$ and $|\mathcal{E}_2\rangle$. It should be noted that the Mandel's Q parameters also have the "holes" on the centre of the states $|\mathcal{E}_1\rangle$ and $|\mathcal{E}_2\rangle$ as shown in the figure. The reason is attributed to the coupling between the states $|\mathcal{E}_1\rangle$ and $|\mathcal{E}_2\rangle$. Clearly, as the increase of the intensity of the field, the absorption peaks broaden due to the power broadening.

The results of the line shape and the Mandel's Q parameter to orthogonal dipole moments of the states $|\mathcal{E}_1\rangle$ and $|\mathcal{E}_2\rangle$ are shown in the right column in Fig. 7. In this case, the interference ways between the states $|\mathcal{E}_1\rangle$ and $|\mathcal{E}_2\rangle$ are turned off, this would lead to non-vanishing absorption at the centre. Also, there is no obvious difference between the orthogonal case and the parallel case at low intensity of laser field.

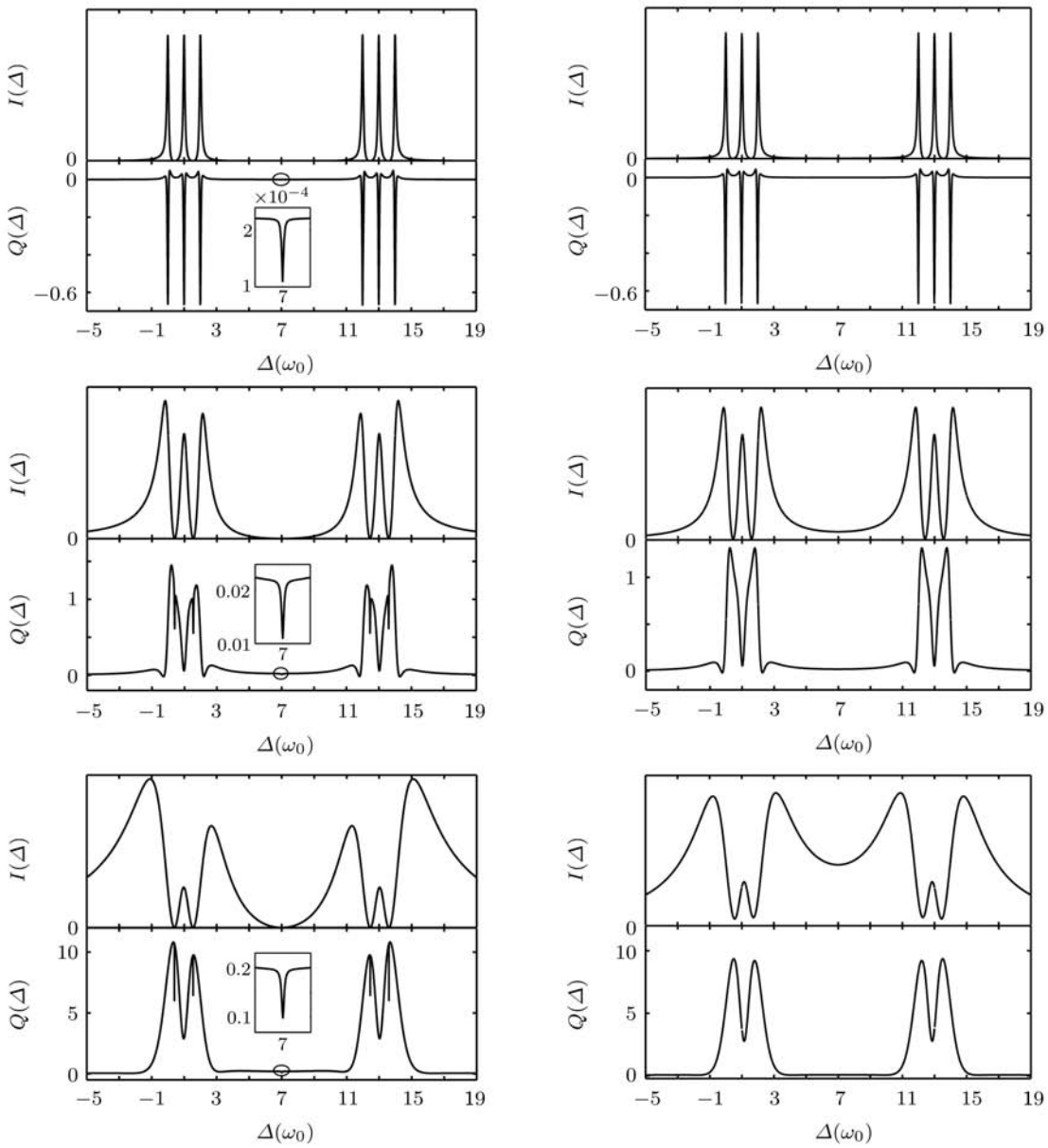


Fig. 7. The line shapes and the Mandel's Q parameters for the three-level-like V-type system. The left column is for the dipole moments parallel case and the right column is for the dipole moments orthogonal case. In our numerical calculations, the Rabi frequencies are equal to 0.05 ω_0 (top panel), 0.5 ω_0 (middle panel), 2.5 ω_0 (bottom panel), and the initial condition is $|\Psi(0)\rangle = |0\rangle$. All the GDCs are 0.05 ω_0, except $\gamma_{ee'} = 0$ ($e = 1, 2, 3$; $e' = 4, 5, 6$) for the dipole moments orthogonal case.

4. Conclusion

In this work, we extended the generating function to the single multi-level quantum system with (quasi-)degenerated levels and studied the statistics of photon emission of the single multi-level quantum system for several cases. The generalized decay constants should be included in the single multi-level quantum system with the degree of (quasi-)degeneracy because of the fail of the secular approximation. The generalized decay constants play an important role in quantum interference and coherence in the dynamical evolution of the system. We verify the generating function approach to reproduce the results of previous work of the line shapes (the first moments), then to extend it to the higher moments (for example, the Mandel's Q parameters, etc.).

The external field can cause the complete absence of absorption or the so-called "dark state" between the excited levels for the case of all the dipole moments parallel. However, for the other cases, it is the different status. We find there exists "sub-beats" for quantum beats of the multi-level quantum system due to quantum interference in the quasi-degenerated states of excited states. The initial state and the dynamical symmetry of the system play an important role in the quantum phenomenon.

Within the present theoretical framework, we could take the further theoretical investigations. For example, we can study the polarized photon emission and their cross correlations by introducing two counting variables. Also, we can investigate the emission probability of the single polarized photon, a pair of polarized photons or the mixed pairs photons, etc. We can control the photon emission of the single multi-level quantum system and generate (different polarized) photons on demand, which has an important application in quantum computation and quantum information.

References

[1] Mukamel S 1995 *Principles of Nonlinear Optical Sepctroscopy* (Oxford: Oxford University Press)
[2] Moerner W E and Kador L 1989 *Phys. Rev. Lett.* **62** 2535
[3] Orrit M and Bernard J 1990 *Phys. Rev. Lett.* **65** 2716
[4] Lu H P, Xun L and Xie X S 1998 *Science* **282** 1877
[5] Moerner W and Orrit M 1999 *Science* **283** 1670
[6] Jelezko F, Lounis B and Orrit M 1997 *J. Chem. Phys.* **107** 1692
[7] Makarov D E and Metiu H 2001 *J. Chem. Phys.* **115** 5989
[8] Cao J S 2006 *J. Phys. Chem.* B **110** 19040
[9] Plenio M B and Knight P L 1998 *Rev. Mod. Phys.* **70** 101
[10] Flindt C, Novotný T, Braggio A, Sassetti M and Jauho A P 2008 *Phys. Rev. Lett.* **100** 150601
[11] Cook R J 1981 *Phys. Rev.* A **23** 1243
[12] Sung J and Silbey R J 2005 *Chem. Phys. Lett.* **415** 10
[13] Shilkerman F and Barkai E 2007 *Phys. Rev. Lett.* **99** 208302
[14] Zheng Y and Brown F L H 2003 *Phys. Rev. Lett.* **90** 238305
[15] Mukamel S 2003 *Phys. Rev.* A **68** 063821
[16] Gopich I and Szabo A 2003 *J. Chem. Phys.* **118** 454
[17] Brown F L H 2003 *Phys. Rev. Lett.* **90** 028302
[18] Bel G and Brown F L H 2009 *Phys. Rev. Lett.* **102** 018303
[19] Sanda F and Mukamel S 2005 *Phys Rev.* A **71** 033807
[20] He Y and Barkai E 2004 *Phys. Rev. Lett.* **93** 068302
[21] Budini A A 2007 *J. Chem. Phys.* **126** 054101
[22] Budini A A 2006 *Phys. Rev.* A **73** 061802
[23] Zheng Y and Brown F L H 2003 *J. Chem. Phys.* **119** 11814
[24] Zheng Y and Brown F L H 2004 *J. Chem. Phys.* **121** 3238
[25] Peng Y, Zheng Y and Brown F L H 2007 *J. Chem. Phys.* **126** 104303
[26] Peng Y and Zheng Y 2008 *Appl. Phys. Lett.* **92** 092120
[27] Han B and Zheng Y 2008 *Phys. Rev.* A **78** 015402
[28] Zheng Y 2008 *J. Chem. Phys.* **129** 246102
[29] Bel G, Zheng Y and Brown F L H 2006 *J. Phys. Chem.* B **110** 19066
[30] Peng Y and Zheng Y 2009 *Phys. Rev.* A **80** 043831
[31] Han B, Ji Z and Zheng Y 2009 *J. Chem. Phys.* **130** 244502
[32] Li X J and Change K 2008 *Appl. Phys. Lett.* **92** 071116
[33] Htoon H, Furis M, Crooker S A, Jeong S and Klimov V I 2008 *Phys. Rev.* B **77** 035328
[34] Gomez E, Aubin S, Orozco L A, Sprouse G D, Tchoukova E I and Safronova M S 2008 *Phys. Rev. Lett.* **100** 172502
[35] Kortyna A, Fiore V and Farrar J 2008 *Phys. Rev.* A **77** 062505
[36] Li G X, Gao T and Zhang Y G 2008 *Chin. Phys.* B **17** 2040
[37] Wang F Y, Shi B S, Lu X S and Guo G C 2008 *Chin. Phys.* B **17** 1798
[38] Zheng Y, Zhang Z and Zhang X 2009 *Acta Phys. Sin.* **58** 8194 (in Chinese)
[39] Peng Y, Zhang X, Zhang Z and Zheng Y 2010 *Acta Phys. Sin.* **59** 1795 (in Chinese)
[40] Wei X G, Wu J H, Sun G X, Shao Z, Kang Z H, Jiang Y and Gao J Y 2005 *Phys. Rev.* A **72** 023806
[41] He Y and Barkai E 2006 *Phys. Chem. Chem. Phys.* **8** 5056
[42] Gopich I and Szabo A 2005 *J. Chem. Phys.* **122** 014707
[43] Gopich I and Szabo A 2006 *J. Chem. Phys.* **124** 154712
[44] Cardimona D A, Raymer M G and Stroud Jr C R 1982 *J. Phys.* B **15** 55
[45] Cardimona D A and Stroud Jr C R 1983 *Phys. Rev.* A **27** 2456
[46] Blum K 1981 *Density Matrix Theory and Applications* 2nd ed. (New York: Plenum)
[47] Milonni P W and Smith W A 1975 *Phys. Rev.* A **11** 814
[48] Rozhkov I and Barkai E 2005 *Phys. Rev.* A **71** 033810
[49] Hegerfeldt G C and Plenio M B 1994 *Quantum Opt.* **6** 15